Supramolecular assemblies tailored by dipyridyl-1,2-4-thiadiazoles: influence of the building blocks in the predictability of the final network

Enrico Podda,[a] Massimiliano Arca,[a] Simon J. Coles,[b] Miriam Crespo Alonso,[a] Francesco Isaia,[a] Anna Pintus,[a] Vito Lippolis,[a] M. Carla Aragoni,[*a]

[a]*Dipartimento di Scienze Chimiche e Geologiche, Università degli Studi di Cagliari, Cittadella Universitaria, SS. 554 bivio Sestu, 09042 Monserrato – Cagliari, Italy.*[b]*UK National Crystallography Service, School of Chemistry, Faculty of Engineering and Physical Sciences, University of Southampton, UK, SO17 1BJ*

E-mail: aragoni@unica.it

Supramolecular assemblies tailored by dipyridyl-1,2-4-thiadiazoles: influence of the building blocks in the predictability of the final network

Coordinatively unsaturated dithiophosphato complex $[Cd((MeO)_2PS_2)_2]$ (**1**) was reacted with the bifunctional ligands 3,5-di-(4-pyridyl)-1,2,4-thiadiazole (**L1**) and 3,5-di-(3-pyridyl)-1,2,4-thiadiazole (**L2**) to give the helicoidal coordination polymer $(\mathbf{1}\cdot\mathbf{L1})_\infty$ and the paddle-wheel dimer $(\mathbf{1}\cdot\mathbf{L2})_2$, both characterized by single crystal X-ray diffraction. A comparison of the structures with the different supramolecular constructs obtained by reacting **L1** and **L2** with differently P-substituted dithiophosphoric Ni^{II} complexes allowed to evaluate the role of the metal ion for the predictable assembly of this class of coordination polymers.

Keywords: coordination polymers (CPs); cadmium; dithiophosphates; XRD; supramolecular networks.

Introduction

The seek in the rational and pre-determined design of crystalline materials has attracted the scientific interest over the past decades.[1–3] The developments in the intriguing field of reticular chemistry allowed chemists to obtain cutting-edge materials such as Charge-Transfer and Proton Transfer compounds,[4–6] Coordination Polymers (CPs),[7] Metal Organic Frameworks (MOFs),[8] and Covalent-Organic Frameworks (COFs)[9] that have been employed in a multitude of applications as different as carbon dioxide capture and conversion,[10] gas storage,[11] catalysis,[12] sensing[13] and photonics.[14,15] Due to the strong dependence of the macroscopic properties of these materials on the reticular scaffold, it is mandatory to understand how the resulting network can be predicted from a meticulous design of the constituent building blocks. The organic linkers can be either charged or neutral in nature and the use of protected metal nodes can lead to more predictable final networks.

In this respect, phosphor-1,1-dithiolates, in particular dithiophosphates (**I**), dithiophosphonates (**II**), and dithiophosphites (**III**) (Scheme 1) have been extensively studied in recent years and have been demonstrated to have a key role in the preparation of coordinatively unsaturated metal complexes that can be used as building blocks in the crystal engineering of CPs.[16–18]

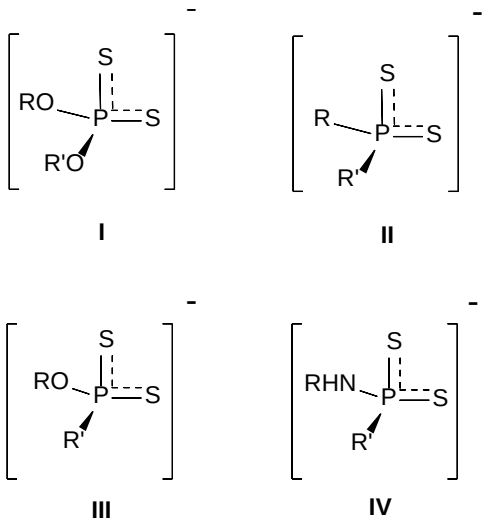

Scheme 1: Phosphor-1,1-dithiolates derivatives: **I** – **IV** = dithiophosphato, dithiophosphinato, dithiophosphonato, and amidodithiophosphonato.

Notably, the class of amidodithiophosphonato (ligand **IV** in Scheme 1) metal complexes remains still unexplored, possibly due to their tendency to hydrolysis at P─N bonds.[19–21] In this respect, we have been developing a synthetic program based on the ability of neutral dithiophosphonato and dithiophosphato Ni^{II} complexes to assemble CPs in combination with a variety of polypyridyl donors, in particular 4,4'-bipyridine and its analogues.[22,23] It was demonstrated that the primary structural motif of these polymers mainly depends on the features of the spacers such as length, rigidity and orientation of the donor atoms, as recently confirmed by the deliberate stereospecific generation of homochiral polymeric helices built from a designed enantiopure binaphthyl-based ligand.[24] The nature of the substituents on the phosphorus atoms impacts on the connection of the polymers through either hydrogen bonds or aromatic interactions, thus influencing the final 2D and 3D-architecture.[24] As a consequence, CPs and 3D

assemblies with different structures and architectures were built up by varying either the bridging ligands or the substituents on the P atom of the initial Ni complexes.[24,25] In this context, we decided to extend our investigations to analogous Cd complexes in order to study the effect of the metal ion on the final structure. In fact, Cd^{II} complexes of **I**-**III** ligands are known to coordinate N-donors to form molecular and polymeric assemblies with coordination numbers that vary between five and six at the central cadmium ion. Following our previous studies on the reactivity of dithiophosphato and dithiophosphonato Ni^{II} complexes towards the bifunctional ligands 3,5-di-(4-pyridyl)-1,2,4-thiadiazole (**L1**) and 3,5-di-(3-pyridyl)-1,2,4-thiadiazole (**L2**), we present here the products obtained by reacting the neutral O-methyl-dithiophosphato Cd^{II} complex (**1**) with di-pyridyl-thiadiazole spacers **L1** and **L2** (see Scheme 2).

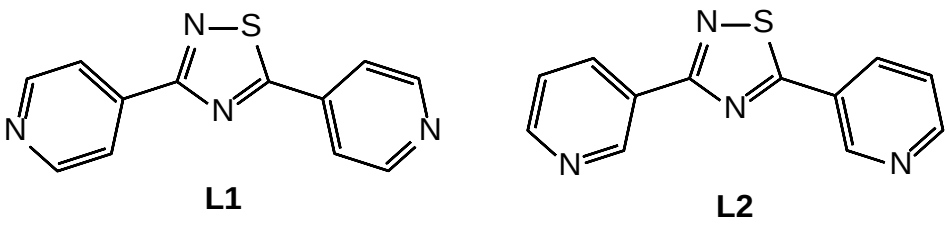

Scheme 2 Formula scheme of 3,5-di-(4-pyridyl)-1,2,4-thiadiazole (**L1**) and 3,5-di-(3-pyridyl)-1,2,4-thiadiazole (**L2**).

Results and discussion

The bifunctional ligands **L1** and **L2** (Scheme 2) feature two pyridyl groups linked by a 1,2,4-thiadiazole ring acting as a rigid, non-reactive spacer.[26] The main feature of these ligands is the existence of different rotational conformations for the pyridyl rings, the most stable being that with the central 1,2,4-thiadiazole ring coplanar to the pyridine moieties.[25]

Ligands **L1** and **L2** were firstly isolated by Meltzer *et al*. in 1955, but their coordination chemistry is still moderately explored and only few papers were published dealing with the use of these ligands in supramolecular chemistry. An overview of the

structurally characterized compounds published until now and the relative supramolecular constructs is summarized in Figure 1.

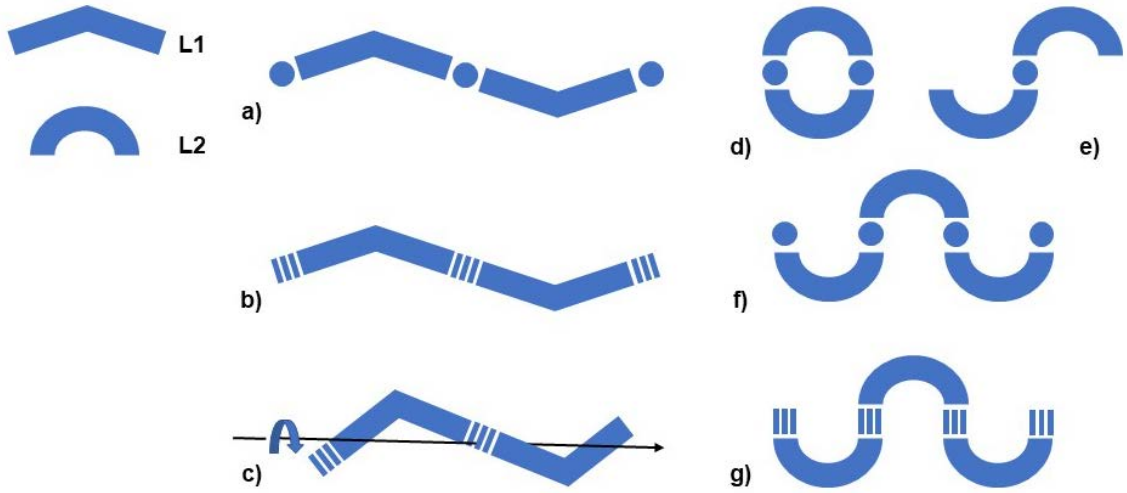

Figure 1: Summary of reported supramolecular constructs found in structurally characterized compounds containing ligands **L1** or **L2**: a) undulated 1D-CPs: EQETOL, EQEVAZ, EQEVIH, EQEVON (ref. 25); b) zig-zag H-bonded 1D-chain: WEDHIY (ref. 28); c) helicoidal H-bonded chain: WEDHOE (ref. 28); d) dimeric paddle-wheel: EQETUR, EQEWAA (ref. 25); e) dimeric complex: TIXTAX (ref 29); f) waving 1D-CPs: EQEVED, EQEVUT (ref. 25); g) waving H-bonded chain WEDGUJ, WEDHEU (ref. 28).

The reactions of **L1** and **L2** with cadmium OMe-dithiophosphato $[Cd((MeO)_2PS_2)_2]$ (**1**) under solvothermal conditions afforded solid, crystalline compounds, which were isolated and identified by means of single crystal X-ray diffraction as the coordination polymer (CP) of formula $(\mathbf{1}\cdot\mathbf{L1})_\infty$ (Figure 2), and the discrete coordination wheel $(\mathbf{1}\cdot\mathbf{L2})_2$ (Figure 5), respectively. Crystallographic data and selected bond lengths and angles are reported in Tables S1 and 1, respectively.

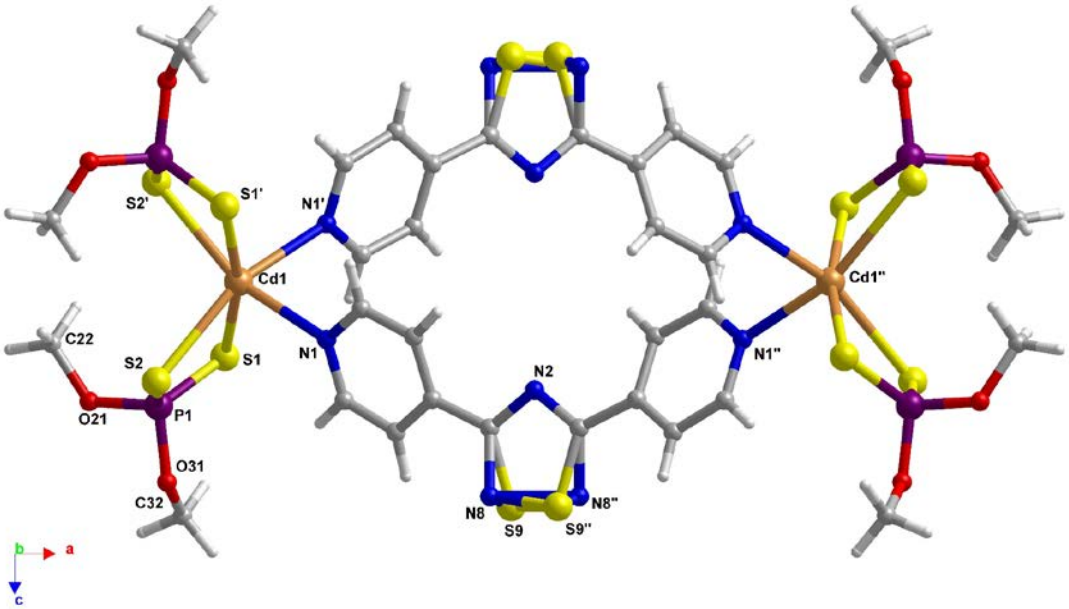

Figure 2: Perspective view along the propagation axis and numbering scheme of the helix (**1**·**L1**)$_\infty$; symmetry codes: ' x, 3/2-y, 1/2-z; " 3/2-x, 2-y, z.

In compound (**1**·**L1**)$_\infty$, the molecules of **L1** are found in two different but essentially superimposable orientations, arising from a 180° rotation of the molecule about the direction passing through the midpoint of the N-S bond and through the remaining nitrogen atom of the penta-atomic ring (Figure 2). Therefore, the nitrogen and the adjacent sulphur atoms show fractional occupancies of 50% for each orientation due to the presence of a two-fold axis passing through the N2 atom. The asymmetric unit of compound (**1**·**L1**)$_\infty$ contains a cadmium ion coordinated by the two sulphur atoms of a dithiophosphato ligand and one nitrogen atom from the half **L1** located on a two-fold axis. The overall geometry is a distorted octahedron with two dithiophosphato ligands coordinated by slightly different Cd─S bonds and two nitrogen atoms belonging to different **L1** spacers. The relevant bond lengths and angles are reported in Table 1. Cd─S distances (2.753 and 2.687 Å) appear to be slightly longer with respect to the mean value of 2.606 Å calculated on the totality of the structures reported in the CCDC.

Table 1 Selected bond lengths (Å), bond and torsion angles (°) and angles between pyridyl ring mean planes (°) for $(\mathbf{1}\cdot\mathbf{L1})_\infty$, $(\mathbf{1}\cdot\mathbf{L2})_2$.

	$(\mathbf{1}\cdot\mathbf{L1})_\infty$		$(\mathbf{1}\cdot\mathbf{L2})_2$
Cd1–S1	2.6873(9)	Cd1–S1	2.6981(10)
Cd1–S2	2.7532(10)	Cd1–S2	2.6638810)
		Cd1-S3	2.7223(11)
		Cd1-S4	2.6836(10)
Cd1–N1	2.388(3)	Cd1–N1	2.386(2)
		Cd1-N14	2.372(3)
P1–S1	1.9868(12)	P1–S1	1.9922(14)
P1–S2	1.9706(12)	P1–S2	1.9958(14)
		P2–S3	1.9761(15)
		P2–S4	2.0020(16)
N1–Cd1–S1	98.55(7)	N1–Cd1–S1	87.03(7)
N1–Cd1–S2	88.37(7)	N1–Cd1–S2	92.34(7)
		N1–Cd1–S3	85.01(7)
		N1–Cd1–S4	94.99(7)
		N14–Cd1–S1	89.06(7)
		N14–Cd1–S2	91.69(7)
		N14–Cd1–S3	90.98(7)
		N14–Cd1–S4	88.90(7)
S1–Cd1–S2	75.06(3)	S1–Cd1–S2	76.85(3)
		S3–Cd1–S4	76.66(3)
S1–P1–S2	113.76(5)	S1–P1–S2	114.29(6)
		S3–P1–S4	114.87(6)
C5-C7-C4-N2	169	C13-C10-C12-N11	168
Py1^Py2	140	C2-C3-C7-N11	21
		Py1^Py2	20

The average Cd─N distance is 2.387 Å, in line with those found in similar CPs.[27] The pyridine rings belonging to spacer **L1** bridge adjacent Cd^{II} ions forming infinite polymeric right-handed helices running along the 010 direction with a Cd···Cd1' pitch of 14.25 Å, equivalent to *b* axis length (Figure 3a). The distance between bridged metal ions in $(\mathbf{1}\cdot\mathbf{L1})_\infty$ is 14.04 Å, which strongly resembles that of 13.70 Å found in the analogous Ni^{II} CP $(\mathbf{1_{Ni}}\cdot\mathbf{L1})_\infty$, reported in Figure 2b for comparison, thus confirming the role of the spacer in determining the primary structure of CPs. This notwithstanding, helices are formed in place of the zig-zag chains found in the corresponding $(\mathbf{1_{Ni}}\cdot\mathbf{L1})_\infty$.[25]

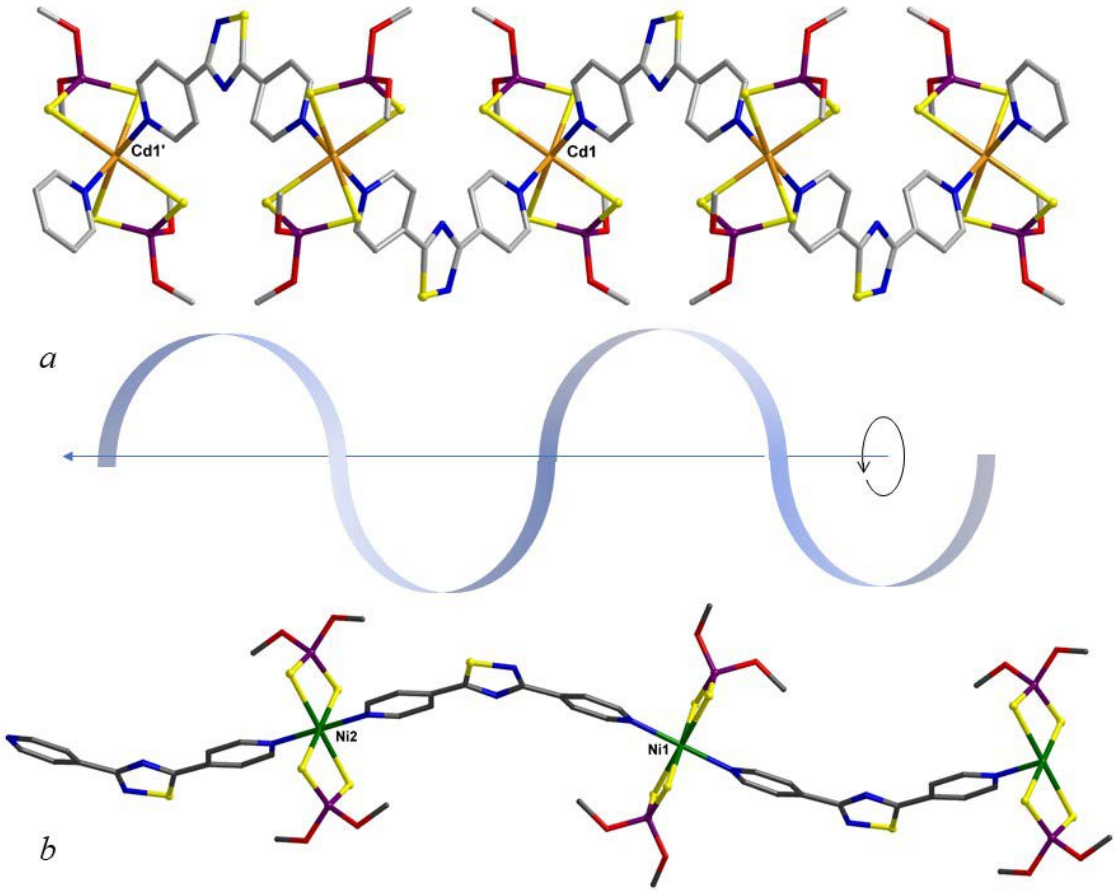

Figure 3 View along the crystallographic *a* axis of a polymeric helix $(\mathbf{1{\cdot}L1})_{\infty}$ (*a*) and an undulated chain of the analogous $(\mathbf{1_{Ni}{\cdot}L1})_{\infty}$ (*b*). For clarity reasons, H-atoms are omitted, and only one orientation of the penta-atomic ring depicted. Symmetry code: ' x, 1+y, z.

A comparison between the two analogous CPs $(\mathbf{1{\cdot}L1})_{\infty}$ and $(\mathbf{1_{Ni}{\cdot}L1})_{\infty}$ evidences that different coordination isomers are formed that feature the bridging **L1** ligands arranged in *cis* (N–Cd–N', 82.18(2)°) and *trans* (N–Ni–N', 180.00(4)°) configuration around the octahedrally coordinated Cd^{II} and Ni^{II} ions, respectively (Figure 3). The ensuing different N─M─N angles result in the formation of helices for $(\mathbf{1{\cdot}L1})_{\infty}$ and chains in the case of $(\mathbf{1_{Ni}{\cdot}L1})_{\infty}$.

Helices running along 010 and 0-10 directions pack interacting to each other through C─H···O H-bonds involving facing OMe P-substituents (C32b─H32d···O21' 2.52, 2.974(9) Å, 108°; ' 0.5+x, y, 1-z; interaction **a** in Figure 4) and C─H ···S short contacts, involving the pyridine rings and the coordinating sulphur atoms (C6─H6···S1" 2.81,

3.489(4) Å, 129°; " x, 1.5-y, 0.5-z; ; interaction **b** in Figure 4), thus leading to the 2D layers shown in Figure 4. Packing views reporting the helices in different colours evidencing the orientation are showed in Figure 1SA and 1SB in ESM.

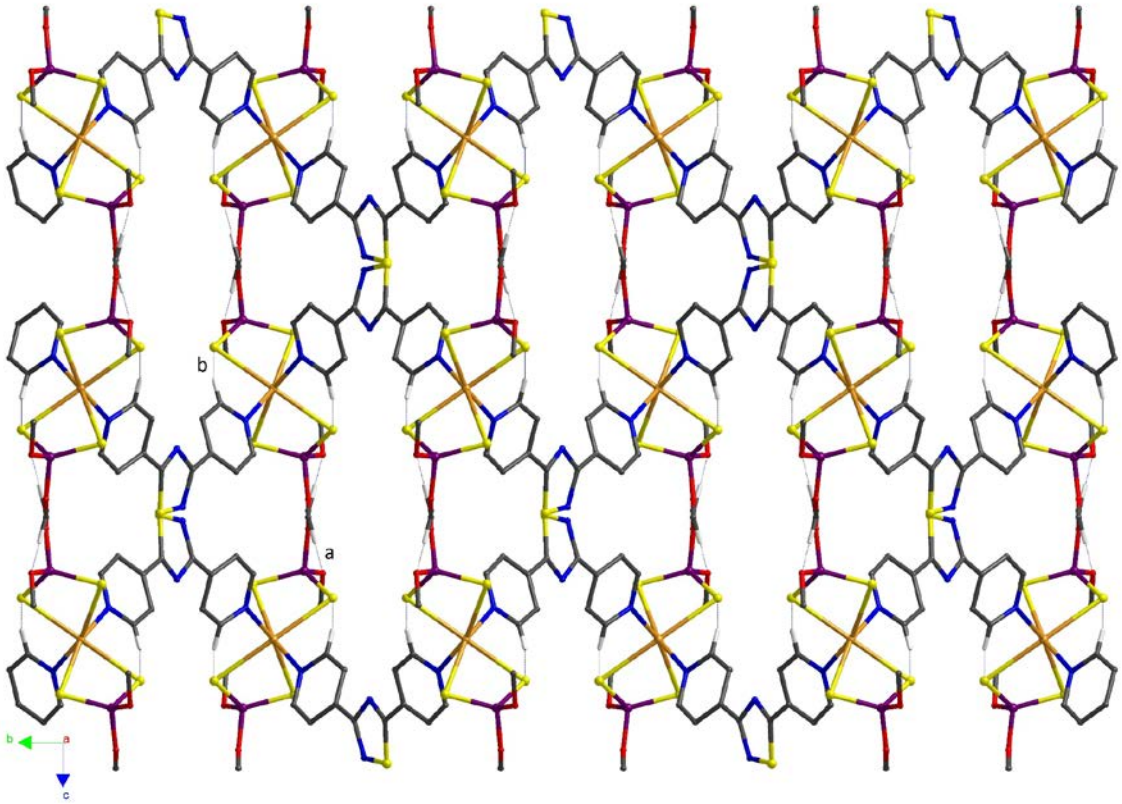

Figure 4: Packing view along the 100 crystallographic direction of helices **(1·L1)**$_\infty$ showing the interactions described in the discussion. For clarity reasons, H-atoms not involved in the showed interactions are omitted and only one orientation of the penta-atomic ring depicted.

It is interesting to note that the interactions involved in the packing of **(1·L1)**$_\infty$ closely resembles those found for **(1$_{Ni}$·L1)**$_\infty$, thus confirming that the packing is mainly governed by the interactions involving the P-substituents, as previously detailed for analogous Ni^{II} CPs featuring different P-substituents.[25]

The reaction of **L2** with coordinatively unsaturated metal ion complexes is known to yield discrete structures,[29] dimeric constructs,[25] and CPs,[25] as summarized in Figure 1. This depends on the possible periplanar and antiperiplanar conformations of **L2** resulting in a different reciprocal orientation of the pyridyl rings (Figure S2 in ESM).

Whilst the **L2** antiperiplanar conformation was found until now only in CPs, the periplanar conformer can lead to different constructs since it can behave as a linker in the dimeric structures and as a divergent linker in CPs (Figure 1). Since the two conformations differ in energy by less than 1 kcal mol^{-1},[25] it was suggested on the base of the structural results, that divergent constructs were favoured by the presence of aromatic P-substituents capable of π-interacting with the aromatic rings of ligand **L2**.[25] The reaction of **1** and **L2** under solvothermal conditions yields the dimer $(\mathbf{1}\cdot\mathbf{L2})_2$, showing a structure very similar to that reported for the analogous nickel complex $(\mathbf{1}_{Ni}\cdot\mathbf{L2})_2$. Ligand units adopt a convergent conformation giving rise to a paddle-wheel structure displaying a distorted octahedral Cd^{II} environment shaped by two dithiosphosphato moieties binding the metal centre at the equatorial positions and two bridging units of **L2** coordinating cadmium ions at their axial positions (Figure 5).

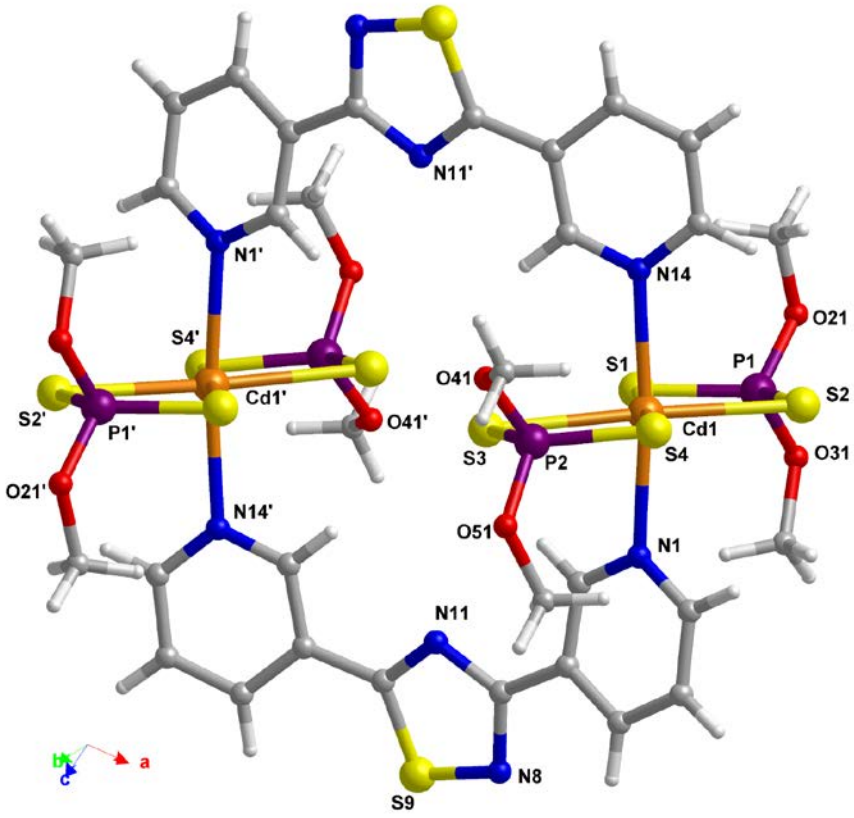

Figure 5: Structure and numbering of the dimer $(\mathbf{1}\cdot\mathbf{L2})_2$; symmetry code: ' 1-x, -y, 1-z.

The asymmetric unit is formed by a half-dimeric molecule, with Cd─S distances ranging from 2.664 to 2.722 Å and Cd─N distances similar to those found in $(\mathbf{1}\cdot\mathbf{L1})_{\infty}$ (Table 1). In the dimer $(\mathbf{1}\cdot\mathbf{L2})_2$, a couple of **L2** spacers bridges two dithiophosphato cadmium complexes through axial coordination generating eicos-atomic planar wheels with openings of about 8 × 8 $Å^2$, and inner Cd ⋯Cd distances of 7.95 Å.

The dimers $(\mathbf{1}\cdot\mathbf{L2})_2$ are arrayed in regular perforated layers assembled by N⋯H and S⋯H interactions (Figure 6a). Symmetry related parallel layers pack in an off-set compact arrangement along the *b* direction showed in Figure 3S. It is interesting to note that no significative differences can be found between $(\mathbf{1}\cdot\mathbf{L2})_2$ and the analogous $(\mathbf{1_{Ni}}\cdot\mathbf{L2})_2$.[25]

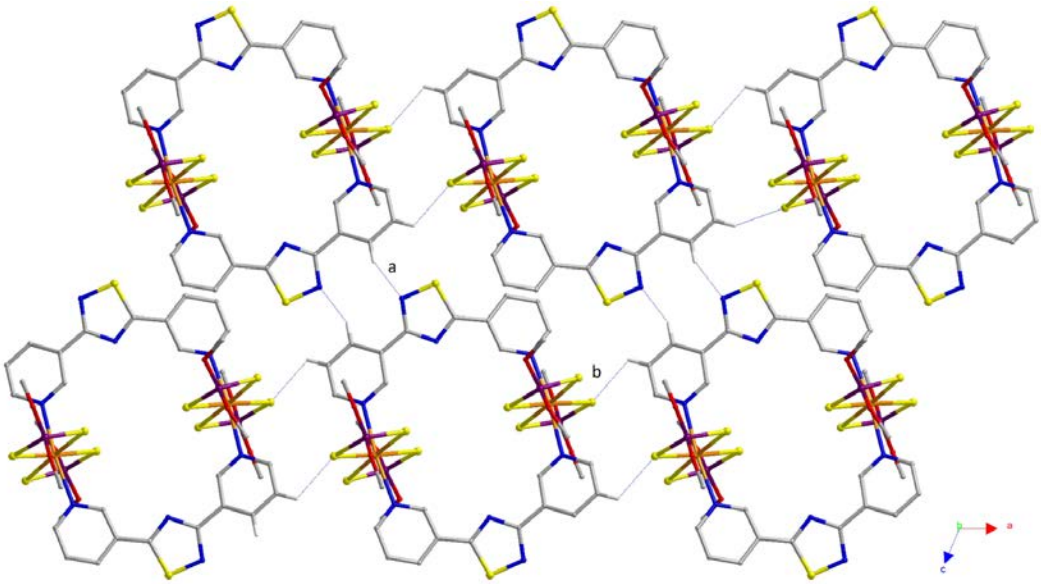

a

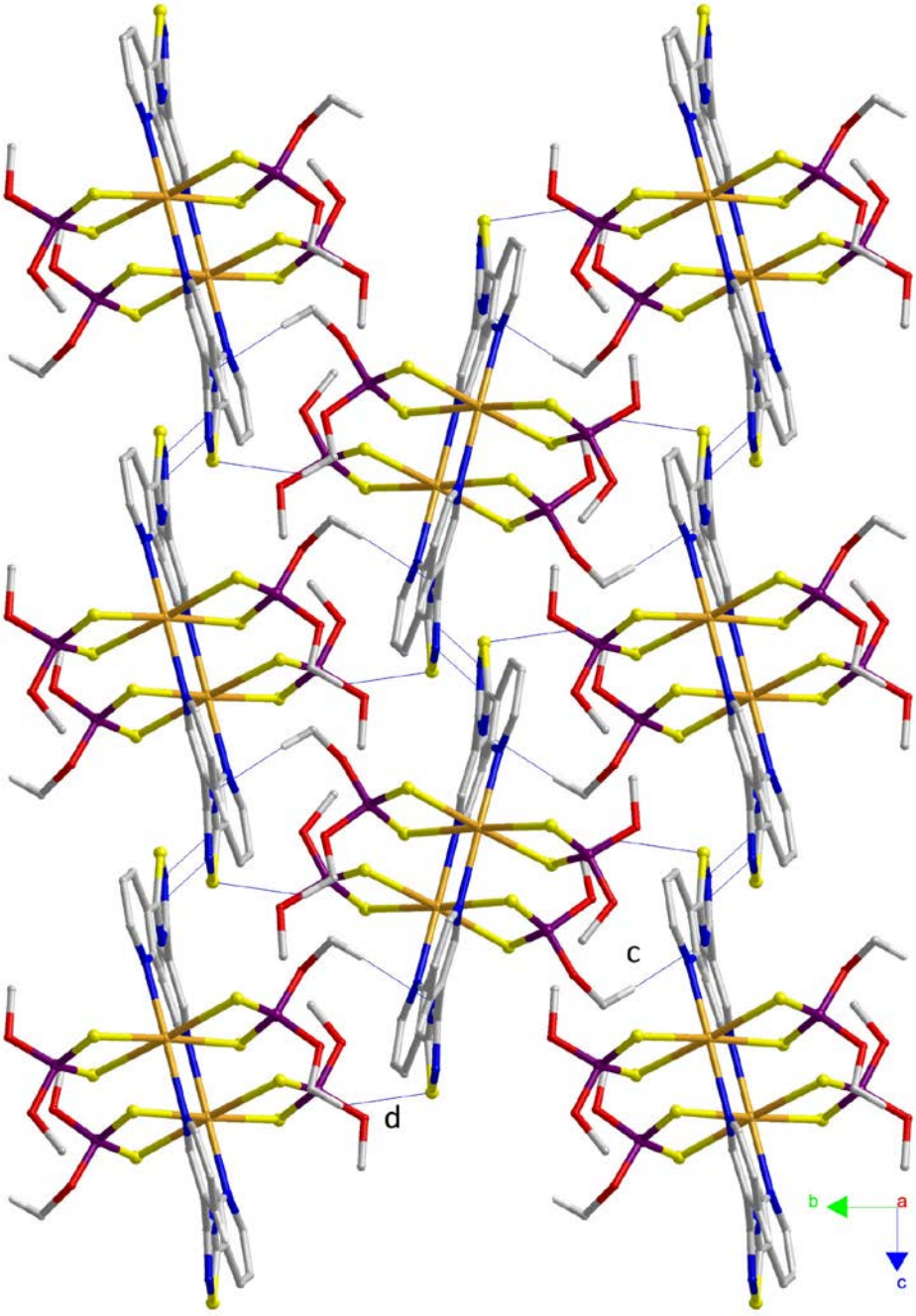

b

Figure 6 Packing views of $(\mathbf{1}\cdot\mathbf{L2})_2$ showing the (*a*) layers formed by interacting dimers along 010 and (*b*) intercalating layers along 100. All the hydrogen atoms with the exception of those involved in the showed interactions have been omitted. Interactions: **a**: C4^{i}–H4^{i}···N8, 2.62, 3.153(5), 116; **b**: C5^{ii}–H5^{ii}···S2, 3.01, 3.633(8), 120; **c**: C42–H42a···N11^{iii}, 2.42, 3.365(5), 164; **d**: C52b^{iv}–H52b^{iv}···S9, 2.83 Å, 3.548(5) Å, 131°. Symmetry codes: ^{i} 2-x, -y, 2-z; ^{ii} 2-x, -y, 1-z; ^{iii} x, 0.5-y, -0.5+z; ^{iv} x, 0.5-y, 0.5+z.

Both the polymer $(\mathbf{1}\cdot\mathbf{L1})_\infty$ and the dimer $(\mathbf{1}\cdot\mathbf{L2})_2$ were further characterized by elemental analysis and FT-IR spectroscopy (see Experimental). In an attempt to evaluate the extent of aggregation between the building blocks in $(\mathbf{1}\cdot\mathbf{L1})_\infty$ and $(\mathbf{1}\cdot\mathbf{L2})_2$, crystalline

samples of both compounds were dissolved in DMSO-d_6 and ^{1}H NMR analysis was performed and the spectra showed in Figures S4 and S5 in ESM. The aromatic portion of the spectra shows peaks peculiar to *para*- and *meta*-substituted pyridyl moieties, ranging from 8.88 to 8.09 and from 9.49 to 7.61 ppm for $(\mathbf{1}\cdot\mathbf{L1})_\infty$ and $(\mathbf{1}\cdot\mathbf{L2})_2$, respectively. Moreover, a doublet centred at 3.51 and 3.47 ppm is attributed to the methoxy moieties involved in $^3J_{PH}$ scalar coupling with the neighbour NMR active phosphorous nuclei found in $(\mathbf{1}\cdot\mathbf{L1})_\infty$ and $(\mathbf{1}\cdot\mathbf{L2})_2$, respectively. A comparison with the spectra of the corresponding pyridyl ligands **L1** and **L2** (Figures S4 and S5) shows that NMR signals are superimposable to the corresponding ones recorded for the free and coordinated ligands in $(\mathbf{1}\cdot\mathbf{L1})_\infty$ and $(\mathbf{1}\cdot\mathbf{L2})_2$.

Conclusions

The reaction of spacers **L1** and **L2** with the dithiophosphato cadmium complex **1** yields to the formation of a polymeric helicoidal coordination polymer $(\mathbf{1}\cdot\mathbf{L1})_\infty$ and a paddle-wheel shaped dimer $(\mathbf{1}\cdot\mathbf{L2})_2$. A comparison with the results obtained by using the same spacers **L1** and **L2** and the analogous dithiophosphato nickel complex $\mathbf{1_{Ni}}$, confirms that **L1** can be used as a spacer for the predictable assembly of 1D-CPs since the orientation of the nitrogen atoms para-positioned in the outwards pyridyl rings of **L1** self-governs the geometry of the resulting supramolecular construct. Notwithstanding the similarities between the outcoming polymers, a role can be found in the nature of the interacting Lewis acid that allows modulating the shape of the resulting polymeric chain, so that smoothly undulated and zig-zag chains were obtained for the protonated ligand $(\mathbf{L1}H^+)_\infty$,[28] and for the analogous $(\mathbf{1_{Ni}}\cdot\mathbf{L1})_\infty$ CP,[25] whereas $(\mathbf{1}\cdot\mathbf{L1})_\infty$ resulted helix-shaped due to the *cis*-isomerism around the metal node, due to the presence of the cadmium ion in the starting dithiophosphato complex. The nature of the interactions between the helices, on the contrary, closely resembles that found in $(\mathbf{1_{Ni}}\cdot\mathbf{L1})_\infty$ CP, thus

confirming the role of P-substituents in governing the final packing.[25] Moreover, the formation of the dimer (**1**·**L2**)$_2$ confirms that convergent constructs can be obtained in the absence P-substituents aromatic in nature.[25] Further investigations are currently ongoing in our laboratories to test the reactivity of several bridging N-donors with phosphor-1,1-dithiolato complexes differing for the nature of the metal ion and P-substituents, with the scope to obtain predictable polymeric networks.

Experimental

Material and Methods

^{1}H NMR measurements were carried out at 25 °C through a Bruker Avance 300 MHz (7.05 T) spectrometer at the operating frequency of 300.13 MHz. Chemical shifts are reported in parts per million (ppm), calibrated to the residual solvent peak set. Elemental analyses were performed with an EA1108 CHNS-O Fisons instrument. FT-Infrared spectra were recorded on a Thermo Nicolet 5700 spectrometer at room temperature using a flow of dried air. Middle IR spectra (resolution 4 cm^{-1}) were recorded as KBr pellets, with a KBr beam-splitter and KBr windows. X-ray structure determinations and crystallographic data for compounds (**1**·**L1**)$_\infty$ and (**1**·**L2**)$_2$ were collected at 120(2) K by means of combined phi and omega scans on a Bruker-Nonius Kappa CCD area detector, situated at the window of a FR591 rotating anode (graphite Mo-K$_\alpha$ radiation, λ = 0.71073Å). The structures were solved by direct methods, SHELXS-97 and refined on F2 using SHELXL-97. Anisotropic displacement parameters were assigned to all non-hydrogen atoms. Hydrogen atoms were included in the refinement, but thermal parameters and geometry were constrained to ride on the atom to which they are bonded. The data were corrected for absorption effects using SADABS V2.10. Structures have been deposited with the Cambridge Crystallographic

Data Centre: deposition numbers waiting for response.

Syntheses

Compounds **L1**, **L2** were synthesized according to a previously reported procedure.[26]

*Synthesis of **1***

A mixture of $Cd(NO_3)_2 \cdot 4H_2O$ (1.542 g, 5.0 mmol) and P_2S_5 (1.114 g, 5.0 mmol) in methyl alcohol (50 mL) was refluxed for 1 hour, and the solvent was then removed under reduced pressure to give a yellow solid (1.777 g, 4.2 mmol, 83 % yield), that was washed with hexane. **1** was obtained as a pale yellow solid. M.p.: 143-145 °C. Elemental analysis calculated (%) for $C_4H_{12}O_4P_2S_4Cd$: C 11.21; H 2.58; S 30.72; found C 11.26; H 2.83; S 30.05. FT-IR (KBr, 4000-400 cm^{-1}): 3504 vw, 2998 w, 2947 mw, 2837 w, 1775 w, 1594 w, 1561 vw, 1499 w, 1435 m, 1385 w, 1307 w, 1257 mw, 1173 s, 1016 s, 800 s, 765 s, 659 s, 541 s cm^{-1}.

*Synthesis of **(1·L1)**$_\infty$*

L1 (12.0 mg; $5 \cdot 10^{-5}$ mol) and **1** (21.3 mg; $5.0 \cdot 10^{-5}$ mol) were suspended in a 1:1 mixture of methanol/chloroform (30 mL) and reacted at 120 °C. After complete dissolution of solids, the mixture was slowly cooled to room temperature and colourless crystals were isolated by filtration. The product was then washed with fresh methanol and dried under vacuum. (17.7 mg; $2.6 \cdot 10^{-5}$ mol; Y = 53 %) Mp: 174-177 °C. FT-IR (KBr, 4000–400 cm^{-1}): 2940w, 2836w, 2361w, 1609m, 1560mw, 1508w, 1468ms, 1415ms, 1338m, 1293w, 1248w, 1228m, 1213m, 1176m, 1132m, 1065m, 1047s, 1016s, 912s, 850m, 840m, 744m, 733m, 709mw, 671w, 660w, 644w, 553m, 524mw, 442m cm^{-1}. elemental analysis calculated (%) for $C_{16}H_{20}CdN_4O_4P_2S_5$: C 28.81, H 3.02, N 8.4, S 24.03 found: C 27.28, H 2.65, N 7.75, S 23.86.

Synthesis of ***(1·L2)***$_2$

L2 (12.0 mg; $5.0 \cdot 10^{-5}$ mol) and **1** (21.3 mg; $5.0 \cdot 10^{-5}$ mol) were suspended in a 1:1 mixture of methanol/chloroform (30 mL) and reacted at 130 °C. After complete dissolution of solids, the mixture was slowly cooled to room temperature and colourless crystals were isolated by filtration. The product was then washed with fresh methanol and dried under vacuum. (11.1 mg; $1.7 \cdot 10^{-5}$ mol; Y = 33 %) Mp: 170 °C. FT-IR (KBr, 4000–400 cm^{-1}): 2940w, 2836w, 2361w, 1638mw, 1599m, 1584mw, 1502w, 1468mw, 1425mw, 1406m, 1338mw, 1304w, 1238w, 1193m, 1173m, 1136m, 1125m, 1012s, 814m, 779ms, 730m, 696m, 664s, 637ms, 588w, 517m, 503m cm^{-1}. Elemental analysis calculated (%) for $C_{16}H_{20}CdN_4O_4P_2S_5$: C 28.81, H 3.02, N 8.4, S 24.03 found: C 29.29, H 2.83, N 8.32, S 24.72.

Acknowledgements

Fondazione di Sardegna (FdS) - Progetti biennali d'Ateneo annualità 2018 – and Università degli Studi di Cagliari are kindly acknowledge for financial support.

References

(1) S. Wuttke, *Angew. Chem. Int. Ed.* **2019**, *58*, 14024–14024.

(2) H. Furukawa, K. E. Cordova, M. O'Keeffe, O. M. Yaghi, *Science* **2013**, *341*, 1230444.

(3) W. L. Leong, J. J. Vittal, *Chem. Rev.* **2011**, *111*, 688–764.

(4) S. Gatfaoui, N. Issaoui, T. Roisnel, H. Marouani, *J. Mol. Struct.* **2019**, *1191*, 183–196.

(5) A. Moghimi, R. Alizadeh, H. Aghabozorg, A. Shockravi, M. C. Aragoni, F. Demartin, F. Isaia, V. Lippolis, A. Harrison, A. Shokrollahi, et al., *J. Mol. Struct.* **2005**, *750*, 166–173.

(6) M. C. Aragoni, M. Arca, F. A. Devillanova, M. B. Hursthouse, S. L. Huth, F. Isaia, V. Lippolis, A. Mancini, H. Ogilvie, *Inorg. Chem. Commun.* **2005**, *8*, 79–

82.

(7) M. Galbiati, N. Motta, M. De Crescenzi, L. Camilli, *Appl. Phys. Rev.* **2019**, *6*, 41310.

(8) A. V Desai, S. Sharma, S. Let, S. K. Ghosh, *Coord. Chem. Rev.* **2019**, *395*, 146–192.

(9) X. Ma, T. F. Scott, *Commun. Chem.* **2018**, *1*, 98.

(10) M. Ding, R. W. Flaig, H.-L. Jiang, O. M. Yaghi, *Chem. Soc. Rev.* **2019**, *48*, 2783–2828.

(11) H. Furukawa, O. M. Yaghi, *J. Am. Chem. Soc.* **2009**, *131*, 8875–83.

(12) A. Dhakshinamoorthy, Z. Li, H. Garcia, *Chem. Soc. Rev.* **2018**, *47*, 8134–8172.

(13) X. Fang, B. Zong, S. Mao, *Nano-Micro Lett.* **2018**, *10*, 64.

(14) Y. Hasegawa, T. Nakanishi, *RSC Adv.* **2015**, *5*, 338–353.

(15) B. Dutta, D. Das, J. Datta, A. Chandra, S. Jana, C. Sinha, P. P. Ray, M. H. Mir, *Inorg. Chem. Front.* **2019**, *6*, 1245–1252.

(16) M. C. Aragoni, M. Arca, F. A. Devillanova, J. R. Ferraro, F. Isaia, F. Lelj, V. Lippolis, G. Verani, *Can. J. Chem.* **2001**, *79*, 1483–1491.

(17) M. C. Aragoni, M. Arca, F. Demartin, F. A. Devillanova, C. Graiff, F. Isaia, V. Lippolis, A. Tiripicchio, G. Verani, *Eur. J. Inorg. Chem.* **2000**, *2000*, 2239–2244.

(18) W. E. van Zyl, J. D. Woollins, *Coord. Chem. Rev.* **2013**, *257*, 718–731.

(19) E. Podda, M. Arca, G. Atzeni, S. J. Coles, A. Ibba, F. Isaia, V. Lippolis, G. Orrù, J. B. Orton, A. Pintus, E. Tuveri, M. C. Aragoni, *Under Submission.* **n.d.**

(20) B. E. Alexander, S. J. Coles, B. C. Fox, T. F. Khan, J. Maliszewski, A. Perry, M. B. Pitak, M. Whiteman, M. E. Wood, *Medchemcomm* **2015**, *6*, 1649–1655.

(21) J. J. Woods, J. Cao, A. R. Lippert, J. J. Wilson, *J. Am. Chem. Soc.* **2018**, *140*, 12383–12387.

(22) M. C. Aragoni, M. Arca, V. Cabras, S. J. Coles, G. Ennas, F. Isaia, R. Lai, V. Lippolis, E. Podda, *Supramol. Chem.* **2017**, *29*, 853–864.

(23) V. Cabras, M. C. Aragoni, S. J. Coles, R. Lai, M. Pilloni, E. Podda, A. Scano, G. Ennas, *Supramol. Chem.* **2017**, *29*, 865–874.

(24) M. Crespo Alonso, M. Arca, F. Isaia, R. Lai, V. Lippolis, S. K. Callear, M. Caricato, D. Pasini, S. J. Coles, M. C. Aragoni, *CrystEngComm* **2014**, *16*, 8582–8590.

(25) M. C. Aragoni, M. Arca, S. J. Coles, M. Crespo Alonso, S. L. Coles (née Huth), R. P. Davies, M. B. Hursthouse, F. Isaia, R. Lai, V. Lippolis, *CrystEngComm* **2016**, *18*, 5620–5629.

(26) R. I. Meltzer, A. D. Lewis, J. A. King, *J. Am. Chem. Soc.* **1955**, *77*, 4062–4066.

(27) C. S. Lai, E. R. T. Tiekink, *CrystEngComm* **2004**, *6*, 593–605.

(28) M. C. Aragoni, M. Arca, C. Caltagirone, C. Castellano, F. Demartin, A. Garau, F. Isaia, V. Lippolis, R. Montis, A. Pintus, *CrystEngComm* **2012**, *14*, 5809–5823.

(29) I. Ondrejkovicova, R. Uhrecky, M. Koman, Z. Faberova, D. Lackova, J. Mrozinsky, B. Kalinska, Z. Padelkova, *Inorg. Chim. Acta* **2014**, *414*, 33-38.